Polymer 50 (2009) 1015–1024

Contents lists available at ScienceDirect

Polymer

journal homepage: www.elsevier.com/locate/polymer

Electric field enhanced sample preparation for synthetic polymer MALDI-TOF mass spectrometry via Induction Based Fluidics (IBF)

Brent Hilker [a], Kevin J. Clifford [a], Andrew D. Sauter, Jr. [b], Andrew D. Sauter, III [b], Ted Gauthier [a], Julie P. Harmon [a,*]

[a] Department of Chemistry, University of South Florida, 4202 East Fowler Avenue, CHE 205, Tampa, FL 33620, USA
[b] Nanoliter LLC, 217 Garfield Drive, Henderson, NV 89074, USA

ARTICLE INFO

Article history:
Received 23 September 2008
Received in revised form
19 December 2008
Accepted 23 December 2008
Available online 27 December 2008

Keywords:
Polymer
IBF
MALDI

ABSTRACT

MALDI-TOF mass spectroscopy is used in the characterization of synthetic polymers. MALDI allows for determination of: modal, most probable peak (M_P), molecular number average (M_N), molecular weight average (M_W), polydispersity (PD), and polymer spread (P_{SP}). We evaluate a new sample preparation method using Induction Based Fluidics (IBF) to kinetically launch and direct nanoliter volumes to a target without contact. IBF offers signal improvement via field enhanced crystallization. This is the first paper to discuss filed enhanced crystallization in MALDI sample preparation. IBF can increase signal/noise (S/N) and signal intensity for polystyrene (PS), poly(methyl methacrylate) (PMMA), and poly(ethylene glycol) (PEG) across a mass range of 2500–92,000 Da showing more accurate P_{SP}. Increases in S/N range up to: 279% for PS, 140% for PMMA, and 660% for PEG. Signal intensities increased up to: 438% for PS, 115% for PMMA, and 166% for PEG. Cross-polarization microscopy indicates dramatic morphology differences between IBF and micropipette. Finally, we speculate as to why IBF nanoliter depositions afford higher S/N values in experiments conducted in different instrumental configurations even without optimization.

1. Introduction

Matrix assisted laser desorption/ionization time-of-flight (MALDI-TOF) mass spectroscopy is currently widely used in the structural characterization of synthetic polymers. Polymer characterization by MALDI allows for the rapid determination of: modal, most probable peak (M_P), molecular number average (M_N) (Eq. (1)), molecular weight average (M_W) (Eq. (2)), polydispersity (PD) (Eq. (3)), and polymer spread (P_{SP}) (Eq. (4)) [1–4].

$$M_N = \frac{\sum N_x M_x}{\sum N_x} \tag{1}$$

and

$$M_W = \frac{\sum N_x M_x^2}{\sum N_x M_x} \tag{2}$$

where M_x is the molecular weight of a molecule corresponding to a degree of polymerization x, N_x the total number of molecules of length x, M_N the number average molecular weight, and M_W is the weight average molecular weight.

$$PD = \frac{M_W}{M_N} \tag{3}$$

$$P_{SP} = \frac{\left|\Delta w_{1/2}\right|}{MM} \tag{4}$$

PD is used to estimate the breadth of the distribution by the ratio of molecular weight average to molecular number average. P_{SP} defined by Tatro et al. is the width of the spectrum without bias being caused by the magnitude of the molecular weight of the polymer [3]. To calculate P_{SP} a Gaussian distribution is formed by aggregating the observed peaks about the M_P, where $\Delta w_{1/2}$ is the absolute value difference of the width at half height, MM is the molar mass of the monomer repeat unit. This allows for the determination of the number of monomer units within one standard deviation from the M_P, which can make classification and comparison simpler.

Preparation of the MALDI target is a crucial step in obtaining optimum spectra. In 2006, G. Montaudo et al. reviewed advances in sample preparation techniques that improved high mass resolution, end group identification, and sequence analysis [1]. These

* Corresponding author. Tel.: +1 813 974 3397.
E-mail address: harmon@cas.usf.edu (J.P. Harmon).

0032-3861/$ – see front matter © 2008 Elsevier Ltd. All rights reserved.
doi:10.1016/j.polymer.2008.12.041

improvements have led to more accurate characterizations of polymers. Additional improvements in MALDI sample preparation techniques such as layering, solvent-free sample preparation, surface preparations/coatings, and the addition of sugars have also proven to be excellent methods for MALDI sample preparation improvement for low molecular weight polymers/proteins yielding increased signal/noise (S/N) and resolution (R_s) [5–12].

In 2008 Tu et al. reported a novel sample preparation technique for ionic liquid matrices (ILE) and conventional solid matrices using an intact protein bradykinin (BK), a 9-amino acid peptide chain with a MM of 1060.21 Da, that employed the use of Induction Based Fluidics (IBF) to deposit nanoliter volumes [13]. This patented 'nanoliter' delivery system, Fig. 1, is effectively a microliter syringe that uses electric induction in a process termed Induction Based Fluidics (IBF) to transport and optionally treat liquids [14].

In IBF, a charge is induced on the liquid by passing the fluid through an electric field, inductively, not conductively as in electrospray ionization (ESI) [14,15]. As such, in IBF there are no faradaic processes, only capacitance based ones, unlike ESI. Therefore, the inductive charging process is elegant in that it performs no unwanted electrochemistry, keeping the analyte intact [15]. The physics behind IBF shows that unlike piezoelectric, sound, or other technologies that are applied to transport liquids at low volumes, IBF kinetically launches drops to targets and can dynamically direct the liquids to targets in flight [14,15]. Tu et al. [13], had shown, with equal molar concentrations of analyte, even if the same volume is dispensed the sample planar area of IBF depositions is smaller. This result creates a more spatially concentrated sample (more hot spots) using IBF which generated improved MALDI data. This study also reported that nanoliter quantities of ionic liquid matrices and solid matrices exhibit major improvement in both MALDI sensitivity (ca. 10×) and reproducibility (ca. 5×) using IBF for the analysis of proteins [13]. Additionally, Tu et al. reported seeing a 40% increase in signal enhancement from IBF over micropipette depositions utilizing conventional solid matrices and showed IBF improved the signal of BK. Over the last decade, our laboratory has studied the alignment of polymer molecules in electric fields, via dielectric spectroscopy (DEA) [16–22], and this prompted us to delve deeper into the reason for Tu's results and to focus on using IBF to improve the MALDI signals of synthetic polymers.

It is widely accepted that MALDI sample uniformity greatly enhances the quality of MALDI spectra. A review by Hoteling et al. correlated signal-to-noise ratio with the solubility of matrix and analyte [23]. Shot-to-shot and spectrum-to-spectrum variability was shown to arise from "sweet spots" that formed as a result of segregation of the analyte from the matrix making signals less homogenous which lowers signal quality and intensity. Hanton and Owens [24] report, in addition to the solubility in the liquid phase, the relative rate of precipitation of the matrix and analyte from the combined termed 'solid-phase' solubility is also important for obtaining high quality MALDI spectra. Solid-phase solubility relates to the relative positions and orientations of analyte, ionization agent, and matrix as these precipitated alignments are also important to obtain good polymer MALDI signals [24].

In addition to the smaller more uniform sample size deposits (pL to nL) produced by the nanoliter IBF, the induced field used in sample preparation has an additional benefit with regard to sample segregation. Studies have shown that an induced electric field has the beneficial effect of increasing the solubility of binary, polymer–solvent, and polymer–polymer solutions [25–30]. The induced electric field may reduce segregation and improve solid-phase solubility resulting in beneficially enhanced spectra.

In order to evaluate the benefit of Induction Based Fluidic (IBF) depositions, we applied this sample preparation technique to: (1) three common polymer standards, Fig. 2, (2) a mass rage of polymers ranging from ca. 2500 to ca. 92,000 Da and (3) different matrices and ion sources. Polymers generally exhibit varying degrees of crystallinity and amorphous behavior. The morphology of the polymer standards used may be important to distinguish when evaluating IBF results; polystyrene and poly(methyl methacrylate) are amorphous while poly(ethylene glycol) is semi-crystalline (at low molecular weights).

It has been reported that micropipette 'dried droplet' polymer depositions have high local deposition variability and this variability leads to less reproducible signals [31,32]. A consequence of this heterogeneity of deposition is that characteristic data (M_N and M_W) have high degrees of variance and are not accurate enough for polymer classification. The need for accurate polymer characterization has led to expensive, yet accurate and precise methods such as electrospray ionization (ESI), a conductive technique which sometimes can fragment analytes and gel permeation chromatography (GPC) which is a relative standard and not applicable to all synthetic polymers. IBF is evaluated here as an additional platform to deliver accurate and precise characteristic data.

We also compared the morphologies of IBF and micropipette depositions, using cross-polarization microscopy. Images obtained show discontinuous crystallization for micropipette depositions that may be caused by dissimilar rates of evaporation, thickness of deposition, or altered crystal lattice morphology. These dissimilar crystalline areas are still being investigated. It has long been accepted from previous research that smaller homogenous crystals are the key to produce enhanced MALDI signals [32,33]. We offer evidence to the contrary through the coupling of cross-polarization images with MALDI spectra that result in larger more dense crystal matrices produced via IBF.

With all of these observations, we speculate that nanoliter-IBF depositions in addition to increasing spatial concentration,

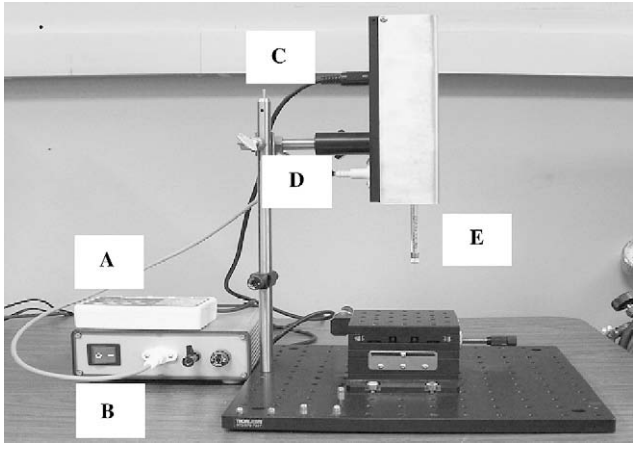

Fig. 1. Nanoliter Induction Based Fluidics (IBF) apparatus: (A) stepper motor controller; (B) nanoliter induction power unit; (C) stepper motor; (D) nanoliter LLC programmable inductor; (E) 10 μL Hamilton removable needle syringe with fused silica needle (i.d. 50/o.d. 150 μm) length 3.5 cm.

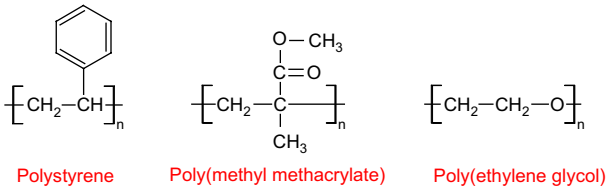

Fig. 2. Structures of polymer standards utilized.

reducing chemical noise, and other complications such as ion clusters, that, in fact, the electric field in IBF *itself* may, in part, be responsible for enhancing the MALDI signal observed by us for synthetic polymers and others for proteins and peptides.

2. Experimental

2.1. Samples and reagents

2.1.1. MALDI reagents

MALDI-TOF-MS analysis was performed on five synthetic polymer samples: (1) a 2300 Da polystyrene sample (Scientific Polymer Products Inc., Ontario, Canada), (2) a 5000 Da poly(ethylene glycol) sample (NIST supplied: Scientific Polymer Cat #500 Case 9004-74-4, Gaithersburg, MD), (3) a 6550 Da polystyrene sample (NIST SRM 1487, Gaithersburg, MD), (4) a 10,600 Da poly(methyl methacrylate) sample (NIST, Gaithersburg, MD), and (5) a 92,600 Da polystyrene sample (American Polymer Standards Corp., Mentor, Ohio, USA). Matrices used in these experiments were retinoic acid (RA) (Sigma Aldrich, St. Louis, MO), 1,1,4,4-tetraphenyl-1,3-butadiene (TPB) (Aldrich Chem Co., Milwaukee, WI), dithranol (Sigma Aldrich, St. Louis, MO), and 2,5-dihydroxybenzoic acid (DHB) (Sigma Aldrich, St. Louis, MO) that was purified by recrystallization using 18.2 $\Omega\,cm^{-1}$ deionized H_2O to remove excess sodium from manufacture source. Salts used in these experiments were sodium trifluoroacetate (NaTFA) and silver trifluoroacetate (AgTFA) (Sigma Aldrich, St. Louis, MO). The solvent used was tetrahydrofuran (THF) HPLC grade (Fischer Chemicals Fair Lawn, New Jersey, USA).

2.2. Sample recipes and preparation

2.2.1. MALDI recipes

The six synthetic polymer samples were prepared using THF as the solvent in the following manner: (1) (PS-2-RA) 5 mg/mL polystyrene (M_N 2300, M_W 2514), 40 mg/mL RA, 5 mg/mL AgTFA. (2) (PS-2) 5 mg/mL polystyrene (M_N 2300, M_W 2514), 45 mg/mL TPB, 5 mg/mL AgTFA. (3) (PEG-5) 5 mg/mL poly(ethylene glycol) 5000 Da, 40 mg/mL dithranol, 5 mg/mL NaTFA. (4) (PS-6) 5 mg/mL polystyrene (M_N 6550), 45 mg/mL TPB, 5 mg/mL AgTFA. (5) (PMMA-10.6) 5 mg/mL poly(methyl methacrylate) (M_N 10,600), 40 mg/mL DHB, 5 mg/mL NaTFA. (6) (PS-92) 7 mg/mL polystyrene (M_N 92,600, M_W 95,050, M_P 94,400), 45 mg/mL TPB, 5 mg/mL AgTFA. All recipes were mixed in [1:10:1] ratio, respectively.

Samples were deposited onto MALDI targets using an Eppendorf 0.1–2.5 μL micropipettor (MP) in sizes ranging 100–500 nL, nanoliter Induction Based Fluidics (IBF) device in sizes ranging 100–500 nL, and KDS-100 single syringe basic infusion pump (SP) (Holliston, MA) size of 100 nL.

2.3. MALDI-TOF-MS

To minimize bias, MALDI-TOF equipment used in this experiment was carefully optimized following guidelines and suggestions reported by Guttman [34] and Wetzal et al. [35] of the polymers division at NIST. Mass calibration, instrument optimization for S/N, matrix and polymer concentration, detector voltage, and time delay were optimized as recommended to ensure high quality and high resolution MALDI spectra [34,35].

Polymer mass spectra were obtained for experiments using samples PS-2, PEG-5, PS-6, and PS-92 using a Voyager-DE™ STR Biospectrometry Workstation (Applied Biosystems, Foster City, CA). Insulin and cytochrome *C* were used as the standards for external calibration. This instrument was equipped with a nitrogen laser (337 nm), and data were obtained by using the linear acquisition mode under delayed extraction conditions. Accelerating voltage was +25 kV and laser shots setting from 750 to 1000. The laser shot values differed due to the physical amount of sample available on the MALDI target. Samples were further individually optimized for signal-to-noise having the following values for grid and delayed extraction: PS-2 (90.0%, 300 ns); PEG-5 (94.5%, 400 ns); PS-6 (95.0%, 350 ns), and PS-92 (96.5%, 700 ns).

Polymer mass spectra for PMMA-10.6 were obtained using a Bruker (Billerica, MA) Reflex II MALDI-TOF-MS. Calibration was performed using Bruker's peptide calibration mix consisting of a multipoint calibration with a quadratic fit using Angiotensin II, Angiotensin I, Substance P, Bombesin, ACTH(1–17) and ACTH(18–39). The acceleration voltage was +25 kV and ions were measured in the linear mode. Delayed extraction was optimized for signal-to-noise for the necessary mass range and the delay (450 ns) was employed for the collection of all data. A nitrogen laser at 337 nm and a 3 ns pulse width was utilized.

2.3.1. MALDI sampling method and data analysis

MALDI spectra consisted of the summation of the total number of ions obtained from 750 to 1000 laser shots. The laser remained in motion to prevent biases in the molecular mass distribution due to heterogeneity regardless of the method of sample application to the MALDI probe. The final MALDI spectrum was an accumulation of the sum of the total laser shots. Resolution (R_s) was calculated by dividing mass (m) by the change in mass at signal half height ($\Delta m_{1/2h}$) (Eq. (5)) accounting for the RMS of the baseline.

$$R_s = m/\left(\Delta m_{1/2h}\right) \tag{5}$$

M_N, M_W, PD, P_{SP}, S/N at M_P, and resolution at M_P were obtained for all sample runs with the Voyager-DE STR. S/N at M_P was obtained for samples run on the Bruker Reflex II. Results were confirmed from additional sample sets.

2.4. Nanoliter induction based fluidic (IBF) device

Fig. 1 shows the nanoliter dispensing device (Nanoliter, LLC, Henderson, Nevada, USA). The device consists of a digital controller, Fig. 1a, a programmable power unit and related electronics and an optional foot pedal, Fig. 1b, housing with stepper motor, Fig. 1c and inductor, Fig. 1d. The device employed a 10 μL Hamilton syringe, Fig. 1e, which was equipped with a fused silica capillary needle, although other types of syringes can be employed in the device.

2.5. Cross-polarization images

A LECA DMRX cross-polarization microscope outfitted with a LEICA DCF 290 imaging camera was used to acquire cross-polarization images of the samples deposited via micropipette and nanoliter IBF device. Via this technique, two polarized planes of light set in extinction allow for the analysis of crystal morphology through the observation of the birefringence of the sample. Similar crystals with similar orientation will appear homogenous when in comparison to one another though their director may have different values. This is a simple tool to find discontinuities and evaluate homogeneity of crystal formations where traditional optical microscopy may not produce an image. Images were processed using Leica Application Suite 3.1 software.

3. Results and discussion

From the work of Tu et al. [13] an apparent counter-intuitive observation that less volume (nL volumes as compared to μL volumes) yields higher signal-to-noise values for proteins,

Table 1
Polystyrene–retinoic acid–AgTFA (PS-2-RA) characterization data.

(PS-2-RA)	M_N	M_W	PD	P_{SP}	(S/N) M_P	R_s at M_P	Laser shots	Intensity M_P
IBF 500 nL	2320	2561	1.10	19	67	342	1000	1026
IBF 250 nL	2360	2561	1.08	17	131	489	750	3901
IBF 100 nL	2358	2595	1.10	17	70	379	750	694
MP 250 nL	2395	2609	1.08	21	34.5	277	750	2904
MP 500 nL	2391	2616	1.09	22	21	319	1000	1116

peptides, and synthetic polymers has been observed. These experiments conducted on different instruments in positive ion linear mode and positive ion reflectron mode suggest that there may be a number of factors contributing to these observations. Tu et al. and this study have shown that IBF has the ability to spatially concentrate depositions, the deposition occupies less planar area. Incoming photons will then have a greater probability of hitting an analyte, matrix "crystal" subsequently producing an analytical ion of interest from use of the IBF method, in direct volume comparison. So the ability of IBF to concentrate analyte in nL spots may increase the probability that any given photon can generate analytical ions of interest.

With a higher density of 'hot spots' one would naturally anticipate that there would be less areas on the target that would generate noise, i.e., those spots devoid of analyte that contains only matrix, that can only produce noise. Karas et al. [36] have discussed the adverse impact of "reneutralizations" caused by "highly charged" clusters ions. We forward here that, in fact, with nL depositions one not only increases the probability to create more analytical ion of interest, but the analytical ion has a much lower probability to be neutralized, as there is simply much less ionized matrix per shot. Therefore, both an increase in ion creation from a spatial perspective and a decrease in ion destruction processes in MALDI steps may increase the signal and reduce the noise when IBF nanoliter depositions are employed in any MALDI configuration.

Furthermore, Debye and Kleboth, in 1962, have shown electric fields increase solubility by reducing the free energy of mixing when an electric field is applied to a binary solution that is in the vicinity of the critical point [25]. This phenomenon was expanded to polymer solutions and further investigated by Wirtz et al. where they concluded that a stationary electric field lowered the coexistence and spinodal curves of a polymer–solvent system, making components more soluble when subjected to an external electric field [26,27]. Moreover an applied external electric field has been shown to alter the morphology of crystallization where precipitates formed under electric field were found to be ca. 10–100 times larger sized [37,38].

3.1. Polystyrene

3.1.1. (PS-2-RA)

Table 1 summarizes data for PS-2-RA obtained from MALDI. Included in this table are number (M_N) and weight (M_W) average, polydispersity (PD), polymer spread (P_{SP}), signal-to-noise (S/N), resolution (R_s) at modal (M_P), laser shots, and intensity [3,39,40].

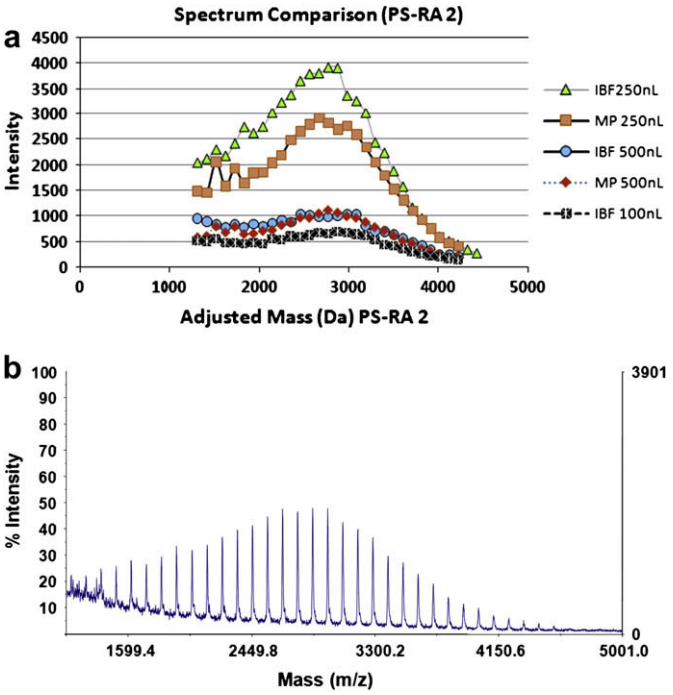

Fig. 3. (a) (PS-2-RA) direct comparison of resolved M/Z peaks for Induction Based Fluidics (IBF) and micropipette (MP) at selected volumes (nL). (b) MALDI spectra (raw signal) PS-2-RA Induction Based Fluidics (IBF) 250 nL deposition.

PS-2-RA data in Table 2 list the percent change in S/N and intensity for volume to volume comparisons of IBF to MP. IBF showed an increase in S/N and R_s.

A comparison of IBF to MP deposition volume of 250 nL shows that IBF improved S/N, an increase of 279%, and improved signal intensity, an increase of 34.3%. These improvements in signal led to a more accurate rendering of P_{SP}. In this case, the P_{SP} became smaller as IBF's increased S/N improved the overall signal quality, Fig. 3a. P_{SP} shows four less monomer repeat units within one standard deviation of the M_P. Fig. 3b shows the raw MALDI spectra obtained for the optimum PS-2-RA IBF deposition volume of 250 nL.

3.1.2. (PS-2)

Table 3 summarizes all the data for PS-2 obtained from MALDI. Included in this table are M_N, M_W, PD, P_{SP}, S/N, R_s at M_P, laser shots, and intensity. PS-2 data in Table 2 list the percent change in volume to volume comparisons between IBF and MP. The IBF method had increased S/N, R_s, and intensity.

Comparing IBF with MP at 250 nL showed an improved S/N and intensity an increase of 75% and 438%, respectively. Furthermore, IBF 100 nL depositions had shown even larger gains in S/N and R_s for this polymer standard. IBF deposition improves the overall signal quality and is seen in Fig. 4a. The better quality signal produced changes P_{SP} value, adding three more monomer units within one standard deviation of the M_P. Fig. 4b shows the raw

Table 2
Change in signal/noise and intensity (%) in volumetric equivalent depositions using IBF method compared to manual pipette/syringe pump for various polymer standards.

	PS-RA-2		PS-2		PS-6		PS-92		PMMA-10.6		PEG-5	
	S/N	Intensity	S/N	Intensity	S/N	Intensity	S/N	Intensity	S/N	Intensity	S/N	Intensity
IBF 500	219%	−8.06%	31.9%	12.5%	15.4%	9.2%	–	–	140%	55%	660%	166.4%
IBF 250	279%	34.3%	75%	438%	69.2%	303.5%	–	–	103%	115%	52.2%	18.1%
IBF 100	–	–	–	–	–	–	190%	128%	–	–	142%	16.9%

Table 3
Polystyrene, TPB, AgTFA (PS-2) characterization data.

(PS-2)	M_N	M_W	PD	P_{SP}	(S/N) M_P	R_s at M_P	Laser shots	Intensity M_P
IBF 500 nL	2361	2599	1.10	18	2723	358	1000	1.80E+04
IBF 250 nL	2258	2545	1.12	19	3186	358	750	4.90E+04
IBF 100 nL	2299	2564	1.11	19	3865	395	750	4.80E+04
MP 500 nL	2415	2640	1.09	16	2065	276	1000	1.60E+04
MP 250 nL	2338	2594	1.10	16	1820	275	750	9.10E+03

Table 4
Polystyrene (6550 Da), TPB, AgTFA (PS-6) characterization data.

(PS-6)	M_N	M_W	PD	P_{SP}	(S/N) M_P	R_s at M_P	Laser shots	Intensity M_P
IBF 500 nL	6525	6660	1.02	20	97.5	790	1000	1248
IBF 250 nL	6587	6770	1.02	23	147.5	551	750	6101
IBF 150 nL	6510	6654	1.02	22	111	472	750	4280
IBF 100 nL	6501	6644	1.02	21	126.6	612	750	3595
MP 500 nL	6517	6650	1.02	19	84.5	672	1000	1142
MP 250 nL	6466	6598	1.02	19	87.2	681	750	1512

MALDI spectra obtained for the PS-2 IBF deposition volume of 100 nL.

3.1.3. (PS-6)

Table 4 summarizes all the data for PS-6 obtained from MALDI. Included in this table are M_N, M_W, PD, P_{SP}, S/N, R_s at M_P, laser shots, and intensity. PS-6 data in Table 2 list the percent change in volume to volume comparisons of IBF and MP. IBF showed an increase in S/N and intensity.

Comparing IBF with MP at 250 nL showed improved S/N and intensity an increase of 69.2% and 303.5%, respectively. IBF deposition improved the overall signal quality as is seen in Fig. 5a. The better quality signal produced changes P_{SP} value, adding four more monomer units within one standard deviation of the M_P. Fig. 5b shows the raw MALDI spectra obtained for the optimum PS-6 IBF deposition volume of 250 nL.

3.1.4. PS-92

Table 5 summarizes data for PS-92 obtained from MALDI for IBF and micropipette depositions. Included in this table are S/N, intensity at M_P, R_s, and P_{SP}. PS-92 data in Table 2 reveal that the IBF deposition (100 nL) had increased S/N and intensity over MP. IBF increased S/N by 190% and intensity by 128%. P_{SP} obtained from the IBF enhanced signal produced via the IBF method indicates a more narrow distribution. Fig. 6a graphically represents the overall signal intensity improvement provided by the IBF deposition method for PS-92. Fig. 6b shows the raw MALDI spectra obtained for the PS-92 IBF deposition volume of 100 nL.

3.2. Poly(methyl methacrylate)

3.2.1. PMMA-10.6

Table 6 summarizes data for PMMA-10.6 obtained from MALDI. Included in this table are S/N and intensity. Table 2 shows the percent increase obtained with the IBF method in volume to volume comparisons. IBF increased S/N by 140% and intensity 55% at 500 nL. IBF also increased S/N by 103% and intensity by 115% at 250 nL.

3.3. Poly(ethylene glycol)

3.3.1. PEG-5

Table 7 summarizes all the data for PEG-5 obtained from MALDI. Included in this table are M_N, M_W, PD, P_{SP}, S/N, R_s at modal M_P, laser shots, and intensity. Data in Table 2 list the percent change in volume to volume comparisons of IBF and MP for PEG-5. IBF showed an increase in S/N and intensity. The most dramatic increase was obtained at 500 nL where IBF showed a gain in S/N of 660% and intensity of 166%.

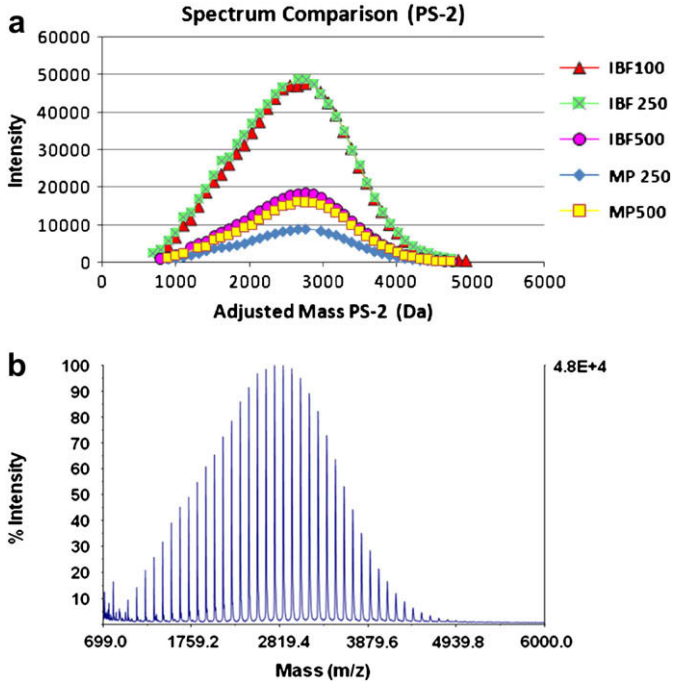

Fig. 4. (a) PS-2 direct comparison of resolved M/Z peaks for Induction Based Fluidics (IBF) and micropipette (MP) at selected volumes (nL). (b) MALDI spectra (raw signal) PS-2 Induction Based Fluidics (IBF) 100 nL deposition.

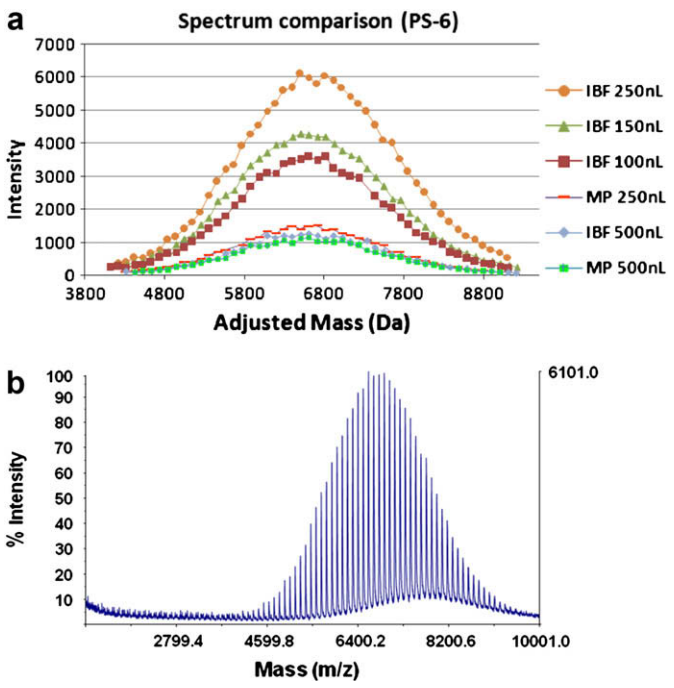

Fig. 5. (a) PS-6 direct comparison of resolved M/Z peaks for Induction Based Fluidics (IBF) and micropipette (MP) at selected volumes (nL). (b) MALDI spectra (raw signal) PS-6 Induction Based Fluidics (IBF) 250 nL deposition.

Table 5
Polystyrene (92,600 Da), TPB, AgTFA (PS-92) characterization data.

PS-92	(S/N) M_P	Intensity M_P	R_s	P_{SP}	Laser shots
IBF 100 nL	26.1	89	14	77	750
MP 100 nL	9	39	14	81	750

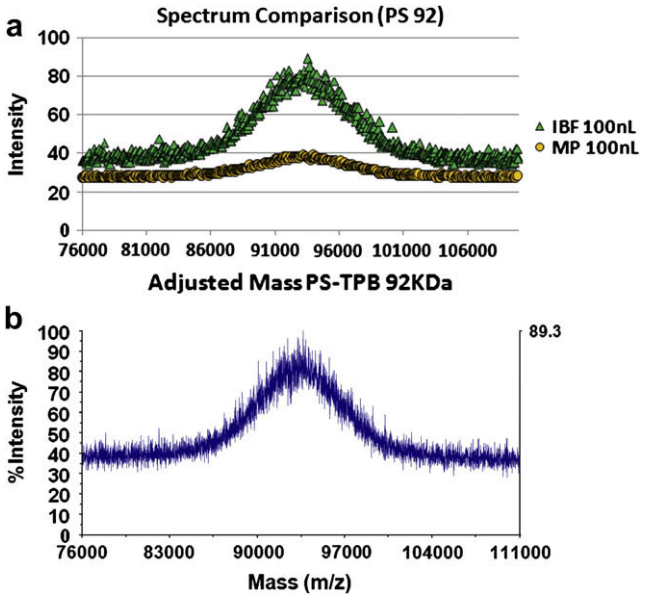

Fig. 6. (a) Polystyrene 92,600 Da (PS-92) direct comparison of signal intensity for resolved *M*/*Z* peaks for Induction Based Fluidics (IBF) and micropipette (MP) at 100 nL. (b) Polystyrene 92,600 Da (raw signal) PS-92 Induction Based Fluidics (IBF) 100 nL deposition.

It should be noted that with increasing volume, IBF yielded enhanced characteristics when compared to micropipette depositions, contrary to previous mentioned data. This observation of both increased S/N and R_s at larger volumes is also counter-intuitive to what has been observed in literature [5,9,10] and may be due to decreased analyte segregation due to the induced electric field [14,15,25–30].

PEG-5 analysis can show the importance of the use of P_{SP} when determining the polymer spread. The PD values for PEG-5 that were generated from the two depositional methods are statistically identical. The P_{SP} method is able to distinguish a difference between the IBF and micropipette depositions while the polydispersity (PD) method reveals no discernable difference. The comparison of the IBF and micropipette depositions at 500 nL reveals that there was a decrease in P_{SP} of 15 less monomer repeat units within one standard deviation of the M_P.

Fig. 7a shows overall signal intensity improvement provided by the IBF deposition method for PEG-5. Fig. 7b shows the raw MALDI spectra obtained for the optimum PEG-5 IBF deposition volume of 500 nL.

Table 6
Poly(methyl methacrylate) (10,600 Da), DHB, NaTFA (PMMA-10.6) characterization data.

PMMA-10.6	(S/N) M_P	Intensity M_P
IBF 500 nL	12	1960
IBF 250 nL	11.8	3450
MP 500 nL	5	1260
MP 250 nL	5.8	1598

Table 7
Poly(ethylene glycol) (5000 Da), dithranol, NaTFA (PEG-5) characterization data.

(PEG-5)	M_N	M_W	PD	P_{SP}	(S/N) M_P	R_s at M_P	Laser shots	Intensity M_P
IBF 500 nL	5378	5418	1.007	26	95	1345	1000	3175
IBF 250 nL	5375	5418	1.008	31	28.3	387	750	1631.5
IBF 100 nL	5376	5419	1.008	32	30.1	451	750	1788
SP 100 nL	5069	5126	1.011	38	12.4	579	750	1529
MP 250 nL	5174	5216	1.008	38	18.6	602	750	1381
MP 500 nL	5099	5164	1.013	41	12.5	334	1000	1192

3.4. Deposition morphology

3.4.1. Amorphous polymer samples

With consistent results showing IBF depositions that yield significant increases in signal quality, our focus turned to the morphology of the deposition. When amorphous polymers are mixed with the crystalline matrix, deposited and dried, the matrix recrystallizes. The extent to which the polymer associates with the matrix influences the quality of the MALDI spectra. Two trends appear when looking at the depositions made with amorphous polymers: (1) IBF depositions yielded larger crystal depositions; (2) IBF depositions having the same volume and concentration when compared to their MP counterparts were more compact, occupying less physical surface area on both the steel AB MALDI plate and glass slides. As previously mentioned, studies have shown and promoted that smaller homogenous crystallization as the preferred and most productive morphology that renders quality MALDI signals [31–33]. In this study, we present evidence from cross-polarization microscopy that directly contradicts the commonly held belief that only smaller homogenous crystals produce quality signal. This contradiction is apparent in the amorphous polymer samples; PS-2-RA, PS-2, 6, PS-92, and PMMA-10.6.

Amorphous samples deposited with micropipette were observed to have smaller homogenous central areas with an outer

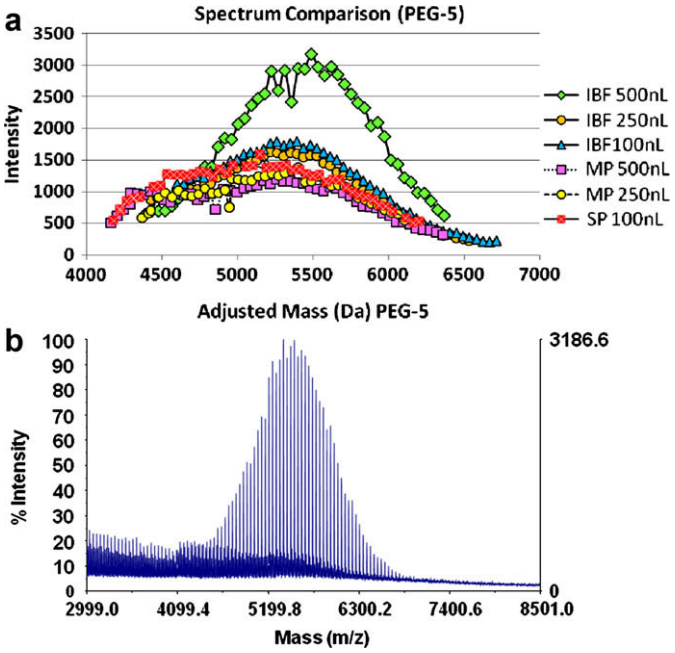

Fig. 7. (a) PEG-5 direct comparison of signal intensity for resolved *M*/*Z* peaks for Induction Based Fluidics (IBF), micropipette (MP) and syringe pump (SP) at selected volumes (nL). (b) MALDI spectra (raw signal) PEG-5 Induction Based Fluidics (IBF) 500 nL deposition.

Table 8
Comparison of deposition volume (nL), radius (r) in μm, and area (μm^2) between IBF and MP on AB steel MALDI plate.

Deposition (nL)	PS-RA-2		PS-2		PS-92		PMMA-10.6		PEG-5	
	r	Area	r	Area	r	Area	r	Area	r	Area
IBF 500	1050	3.46	1150	4.15	–	–	1000	3.14	1550	7.55
IBF 250	1025	3.3	875	2.41	–	–	900	2.54	1125	3.98
IBF 100	875	2.41	550	0.95	625	1.23	650	1.32	800	2.01
MP 500	1550	7.55	1500	7.07	–	–	1300	5.3	2125	14.19
MP 250	1250	4.91	1150	4.15	–	–	1100	3.8	1600	8.04
MP 100	1000	3.14	1000	3.14	875	2.41	750	1.76	1100	3.8

ring that has different, usually larger, crystallization outcrops. This dichotomy seen in the micropipette depositions lends the sample to become heterogeneous and ultimately non-favorable for high quality spectra. Please note when observing the reflected cross-polar images (steel plate) the fact that the MALDI plate itself contains a manufacturer's machine engraved ring that appears in photos as a dark ring ca. 150 μm thick. These rings are placed upon the MALDI plate with sequential numbers for sample recognition.

The substrate effect has been known to change morphology and T_m of polymers based upon the affinity of the polymer to substrate [41]. This effect was considered when taking cross-polarization images on both glass and steel. The same morphological differences aforementioned between IBF and MP methods were noticed on both substrates. This investigation used glass substrate to obtain cross-polar transmission images to more clearly depict what was similarly observed on the AB Steel MALDI target.

3.4.2. Semi-crystalline polymer samples

PEG-5 is the only MALDI sample tested here that is semi-crystalline. This quality may explain why PEG-5 follows a different trend in depositional comparisons. The semi-crystalline PEG-5 yielded two trends: (1) IBF depositions showed smaller homogenous crystallization; (2) IBF depositions were more compact. Micropipette PEG-5 samples have shown a large heterogeneous feather-like ring out cropping where this was not apparent in IBF depositions.

3.4.3. Spatial concentration

All depositions were more spatially concentrated when deposited via IBF. This is to say in volume to volume comparisons of MP and IBF less planar surface area was occupied when IBF depositional technology was employed. Table 8 shows depositional volumes (nL), radius (μm), and area (μm^2) of IBF and MP. About ca 1.5–3.3× greater planar spatial compactness was observed for all depositions using IBF.

Table 9
Polystyrene, retinoic acid, AgTFA. (PS-2-RA) cross-polarization images for IBF and micropipette 250 nL depositions.

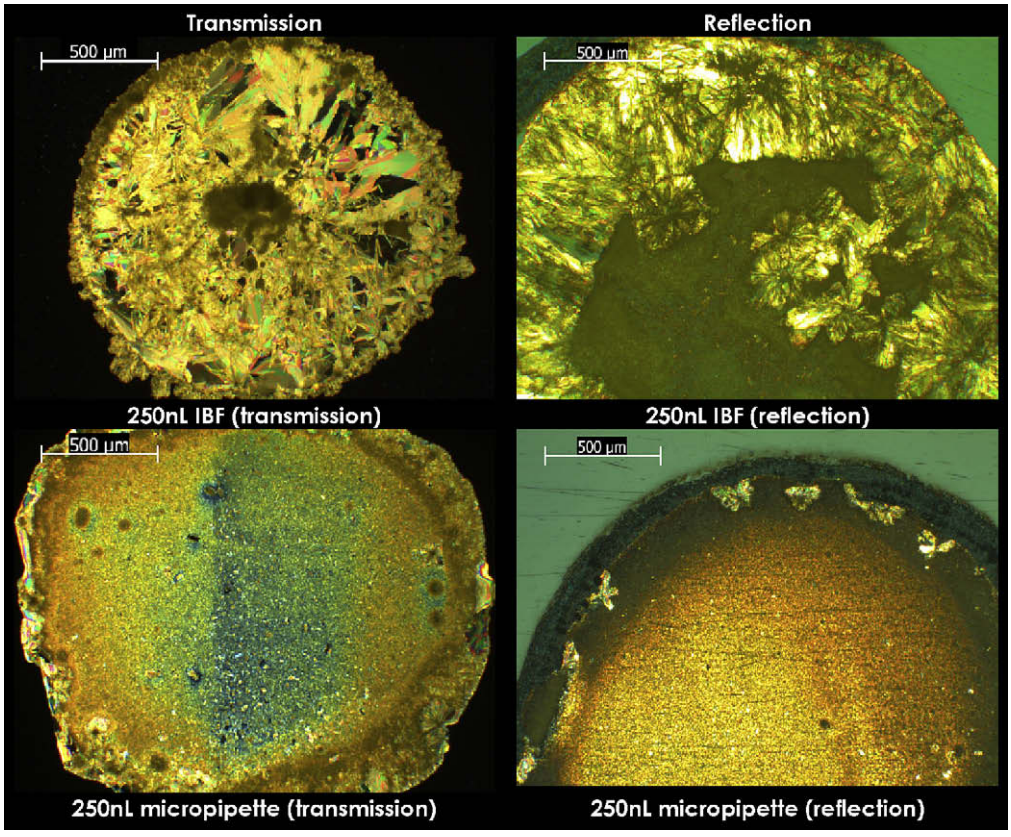

Table 10
Polystyrene (92,600 Da), TPB, AgTFA. (PS-92) cross-polarization images for IBF and micropipette 100 nL depositions.

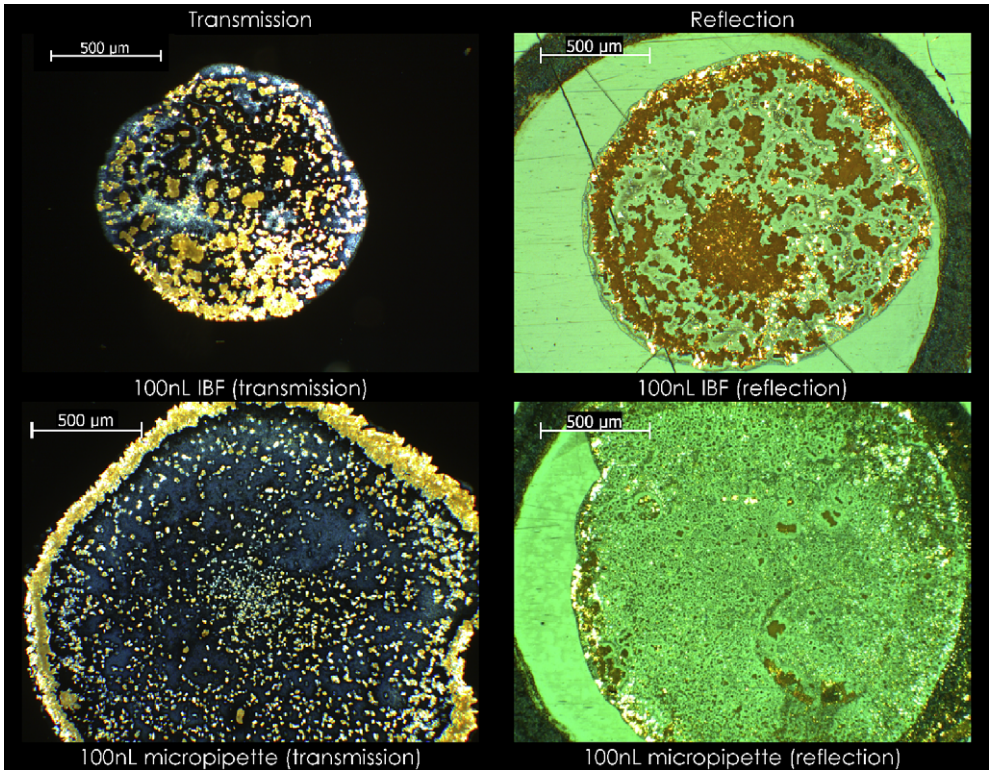

Table 11
Poly(methyl methacrylate) (10,600 Da), dithranol, NaTFA cross-polarization image comparisons of transmission and reflection light of deposition volume 500 nL.

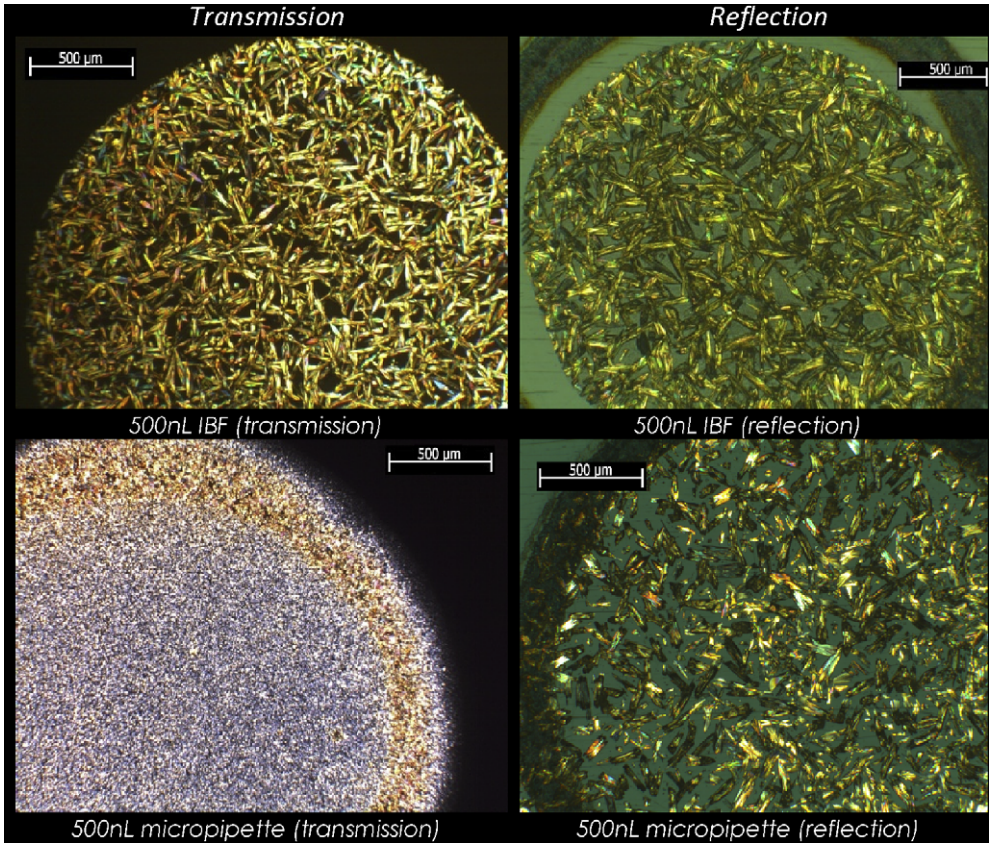

3.5. Cross-polarization images

3.5.1. PS-2-RA

Table 9 shows cross-polarization images obtained in transmission and reflected mode for PS-2-RA. The different substrates (glass and steel) for the two imaging methods (transmission and reflection) show slight differences in area occupied. These differences stem from the hydrophilicity/hydrophobicity differences of each surface. Both substrates, though different, display the same macro-trends previously outlined.

When observing the sample presented here please note that the *Z* direction, sample elevation, could not be simultaneously focused. The darker central crystalline areas in Table 9 (IBF 250), reflection mode, represent a stacking of the same large crystals as seen in the periphery. The IBF 250 nL (transmission mode on glass substrate) allows more light to pass through the sample better revealing the homogenous large crystalline formations in the center that were obscured from view in reflection mode (steel substrate). In comparison, it can be seen that IBF depositions produce larger crystals.

3.5.2. PS-92

Table 10 shows the cross-polarization images obtained in transmission and reflected mode for PS-2-RA. Comparing the two methods reveals that IBF has ca. 2× greater depositional density for reflection (steel plate). IBF shows greater density per unit area over micropipette for PS-92 samples with larger crystal formation.

3.5.3. PMMA-10.6

Cross-polarization images of PMMA-10.6 show a difference in homogeneity for PMMA-10.6 depositions made by micropipette, Table 11. IBF cross-polarization images reveal homogenous crystalline depositions that exhibit greater compactness.

The optimum deposition volume for PMMA-10.6 was 500 nL for both IBF and micropipette yielding the best S/N for each deposition method. The IBF and micropipette 500 nL depositions both show homogenous crystallization. When the micropipette 500 nL deposition is directly compared to IBF 500 nL it is clear that the IBF has greater crystal density per unit area, ca. 1.7× greater crystal density.

A video comparison of the real-time IBF versus micropipette crystallization morphology of PMMA-10.66 at 25, 75, 100, 150, 200, 250, 500, 1000 nL for IBF and 100, 250, 500 nL, for micropipette is available on the World Wide Web at http://chemistry.usf.edu/faculty/harmon/select "*Synthetic Polymer/Matrix Crystallization Video (Windows Media)*".

4. Conclusion

Analysis of synthetic polymers using MALDI, mass range 2500–92,000 Da, can benefit from using nanoliter IBF method for sample preparation. This benefit translates over a wide variety of polymers and ion sources. This sample preparation method shows greater compactness and homogeneity of sample deposition.

With these three polymer standards (PS, PMMA, PEG) we have seen improvements in S/N up to 660% and increases in signal intensity up to 438%. Furthermore, additional MALDI work should be undertaken to investigate the benefit upon R_s from IBF focusing on resolved isotope clusters in reflectron mode.

This device may provide a simple platform to standardize sample preparation, reducing analyst errors while increasing the signal quality. This could lead to increased precision and accuracy when investigations are conducted using MALDI. Additionally, this method may improve inter-laboratory comparisons as a result of removing operator bias at the sample preparation step.

Cross-polar microscopy has shown different morphology between IBF and micropipette depositions. These dramatic differences seen between IBF and micropipette depositions require further study for assessment. Investigations into these differences are underway. Three attractive ideas for these morphological variances are proposed so far: (1) dissimilar rates of evaporation, (2) thickness of deposition, or (3) altered 'electric field' crystal lattice morphology.

Additionally, dramatic morphological differences between IBF and micropipette were captured in real-time movie images. These images are available for viewing in the World Wide Web at http://chemistry.usf.edu/faculty/harmon/select "*Synthetic Polymer/Matrix Crystallization Video (Windows Media)*".

We forward that IBF-nanoliter depositions increase the spatial concentration of analyte compared to μL depositions and hence increase the density of hot spots. This also quite naturally minimizes the area where there is no analyte or cold spots, that can only generate large cluster or other ions that destroy (neutralize) the analytical ion of interest. We further speculate that as nanoliter depositions show improved crystal morphology and no ring structure, evidence of increased solubility, that IBF nanoliter depositions, may also be in fact, "electric field enhanced." As such, it is proposed that a confluence of factors can be invoked to explain the fact that nL-IBF depositions have been observed to increase signal and noise in positive ion data shown here.

Acknowledgements

We would like to extend our thanks to National Institute of Standards and Technology (NIST) Polymers Division, Gaithersburg, MD, USA for providing us with polymer standards for use in this research opportunity. Special thanks to Dr. John M. Koomen, Scientific Director, Proteomics Core Facility at H. Lee Moffit Cancer Center & Research Institute for allowing use of the Voyager-DE™ STR Biospectrometry MALDI Workstation.

References

[1] Montaudo G, Samperi F, Montaudo MS. Prog Polym Sci 2006;31(3):277–357.
[2] Nielen MWF. J Mass Spectrom 1999;18:309–44.
[3] Tatro SR, Baker GR, Fleming R, Harmon JP. Polymer 2002;43(8):2329–35.
[4] Bahr U, Deppe A, Karas M, Hillenkamp F, Giessmann U. Anal Chem 1992;64:2866–9.
[5] Woldegiorgis A, Loewenhielm P, Bjoerk A, Roeraade J. Rapid Commun Mass Spectrom 2004;18(23):2904–12.
[6] Basile F, Kassalainen GE, Ratanathanawong S, Williams SK. Anal Chem 2005;77:3008–12.
[7] Shahgholi M, Garcia BA, Chiu NHL, Heaney PJ, Tang K. Nucleic Acids Res 2001;29(19):e91.
[8] Trimpin S, McEwen CN. J Am Soc Mass Spectrom 2007;18:337–81.
[9] Little DP, Cornish TJ, O'Donnell MJ, Braun A, Cotter RJ, Köster H. Anal Chem 1997;69:4540–6.
[10] Hung KC, Rashidzadeh H, Wang Y, Guo BC. Anal Chem 1998;70:3088–93.
[11] Kussman M, Nordhoff E, Rahbek-Nielsen H, Haebel S, Rossel-Larsen M, Jakobesen L, et al. J Mass Spectrom 1997;32:593–601.
[12] Miliotis T, Kjellstrom S, Nilsson J, Laurell T, Edholm LE, Marko-Varg G. Rapid Commun Mass Spectrom 2002;16:117–26.
[13] Tu T, Sauter Jr AD, Sauter III AD, Gross ML. JASMS 2008;19(8):1086–90.
[14] Sauter AD. Precise electrokinetic delivery of minute volumes of liquid(s). U.S. Patent 6,149,815; November 21, 2000 and US pending patents of A.D. Sauter: 60/574,104; 60/759,787; 60/881,532 and 61/011,178.
[15] Sauter Jr AD. American Laboratory; February 2007.
[16] Clayton LM, Knudsen B, Cinke M, Meyyappan M, Harmon JP. J Nanosci Nanotechnol 2007;7(10):3572.
[17] Mohomed K, Moussy F, Harmon JP. Polymer 2006;47:3856.
[18] Mohomed K, Gerasimov T, Moussy F, Harmon JP. Polymer 2005;46:3847.
[19] Tatro SR, Baker GR, Bisht K, Harmon JP. Polymer 2003;44:167.
[20] Emren S, Liu Y, Newkome G, Harmon JP. J Polym Sci Part B Polym Phys 2001;39:1381.
[21] Emran S, Newkome G, Weis C, Harmon JP. J Polym Sci Part B Polym Phys 1999;37:2025.

[22] Bertolucci P, Harmon JP. Photonic and optoelectronic polymers. In: Jenekhe SA, Wynne KJ, editors. American Chemical Society Symposium Series, vol. 672; 1997. p. 79–97.
[23] Hoteling AJ, Erb WJ, Tyson RJ, Owens KG. Anal Chem 2004;76:5157–64.
[24] Hanton SD, Owens KG. J Am Soc Mass Spectrom 2005;16:1172–80.
[25] Debye P, Kleboth K. J Chem Phys 1965;42(9):3155–62.
[26] Wirtz D, Fuller GG. Phys Rev Lett 1993;71:2236–9.
[27] Wirtz D, Berend K, Fuller GG. Macromolecules 1992;25:7234–46.
[28] Lee JS, Prabu AA, Kim KJ, Park C. Macromolecules 2008;41(10):3598–604.
[29] Shrimada T. Thin Solid Films 2006;515:1568–72.
[30] Onuki A. Europhys Lett 1995;29(8):611–6.
[31] Wetzel SJ, Guttman CM, Flynn KM. Rapid Commun Mass Spectrom 2004;18:1139–46.
[32] Snovida S, Rak-Banville JM, Perreault H. J Am Soc Mass Spectrom 2008;19:1138–46.
[33] Hanton SD, Hyder IZ, Stets JR, Owens KG, Blair WR, Guttman CM, et al. J Am Soc Mass Spectrom 2004;15:168–79.
[34] Guttman CM, Wetzel SJ, Flynn KM, Fanconi BM, VanderHart DL, Wallace WE. Anal Chem 2005;77:4539–48.
[35] Wetzel SJ, Guttman CM, Fylnn KM, Filliben JJ. In: Proceedings of the 52nd ASMS conference on mass spectrometry and allied topics, Nashville, TN, May 23–24; 2004.
[36] Karas M, Gluckmann M, Schafer J. J Mass Spectrom 2000;35(1):1–12.
[37] Dou J, Weijia S, Zhogwei C. Appl Surf Sci 2004;236:57–62.
[38] Sha Y, Zhang F, Li S, Gao X, Xu J, Zuo L. J Mater Sci Technol 2004;20(3):253–6.
[39] Odian G. Principals of polymerization. New Jersey: John Wiley & Sons Inc.; 2004. p. 20–3.
[40] Pasch H, Schrepp W. MALDI-TOF mass spectrometry of synthetic polymers. New York: Springer; 2003. p. 19–22.
[41] Wang Y, Rafailovich M, Sokolov J, Gersappe T, Araki T, Zou Y, et al. Phys Rev Lett 2006;96:028303.